NAGW-3554 5451
NAGW-3838

RADIATION PRESSURE–DRIVEN MAGNETIC DISK WINDS IN BROAD ABSORPTION LINE QUASI-STELLAR OBJECTS

MARTIN DE KOOL

Max Planck Institut für Astrophysik, Karl Schwarzschild Strasse 1, 85740 Garching bei München, Germany; dekool@mpa-garching.mpg.de

AND

MITCHELL C. BEGELMAN[1]

JILA, University of Colorado, Campus Box 440, Boulder, CO 80309-0440; mitch@jila.colorado.edu

ABSTRACT

We explore a model in which QSO broad absorption lines (BALs) are formed in a radiation pressure–driven wind emerging from a magnetized accretion disk. The magnetic field threading the disk material is dragged by the flow and is compressed by the radiation pressure until it is dynamically important and strong enough to contribute to the confinement of the BAL clouds. We construct a simple self-similar model for such radiatively driven magnetized disk winds, in order to explore their properties. It is found that solutions exist for which the entire magnetized flow is confined to a thin wedge over the surface of the disk. For reasonable values of the mass-loss rate, a typical magnetic field strength such that the magnetic pressure is comparable to the inferred gas pressure in BAL clouds, and a moderate amount of internal soft X-ray absorption, we find that the opening angle of the flow is approximately 0.1 rad, in good agreement with the observed covering factor of the broad absorption line region.

Subject headings: accretion, accretion disks — MHD — quasars: absorption lines

1. INTRODUCTION

About 10% of QSOs exhibit strong absorption in the UV resonance lines of highly ionized species like N v, C iv, and Si iv, which are always blueshifted relative to the emission-line rest frame. These lines indicate the presence of outflows from the active nucleus, with velocities ranging up to 0.1c. The properties of these broad absorption lines (BALs) and their interpretation have been reviewed and discussed extensively in, e.g., Weymann, Turnshek, & Christiansen (1985, hereafter WTC); Turnshek (1988); Begelman, de Kool, & Sikora (1991, hereafter BdKS); Weymann et al. (1991); and Hamann, Korista, & Morris (1993). Simple arguments lead to the following model-independent constraints on the physical conditions and geometry of the region in which the BALs are formed (hereafter referred to as the BALR).

1. The ionization parameter of the BAL gas lies in the range $0.01 < U < 1$ (U being the ratio of the number density of photons above the Lyman limit to the hydrogen density) and does not change rapidly with the velocity of the absorbing material. This leads to limits on the density of the BAL gas.

2. Depending on assumptions about line saturation and degree of covering of the continuum source, estimates of the total column density of the BALR range from $N_H \sim 10^{20.5}$ to $N_H \sim 10^{22}$ cm^{-2}.

3. BAL gas occupies only a very small fraction of the volume of the BALR, the filling factors typically being $< 10^{-5}$. Individual BAL clouds are very thin in the direction of our line of sight. Typical dimensions $\sim 10^{11}$ cm can be derived.

4. The BALR has at least some part which is located outside the broad emission-line region (BELR), because the flux in the Lyα BEL is usually significantly reduced as a result of absorp-

tion by the blueshifted N v line, and sometimes the blue wing of the C iv BEL is also absorbed.

5. The absence of observable emission from the high-velocity material seen in absorption indicates that the global covering factor of the BALR is < 0.1. Combined with the fact that 10% of QSOs exhibit BALs, this leads to the conclusion that most QSOs have a BALR.

Apart from these general constraints, relatively little progress has been made in identifying the physical processes underlying the formation of the BALs. The following basic questions still need to be answered:

1. What is the origin of the BAL clouds?
2. What force accelerates the clouds to such high velocities?
3. How do the clouds maintain such a high internal pressure, or in other words, what confines the clouds?

These subjects were already discussed in the first major review of BAL QSOs (WTC). There it was assumed that the confinement had to be caused by a hot gas between the clouds, with a temperature of the order of the Compton temperature of the active galactic nucleus (AGN) radiation field. Since it can easily be shown that such an intercloud medium would exert drag forces on the clouds far in excess of anything achievable by radiation pressure, it was conjectured that these drag forces had to be responsible for the acceleration, the hot medium being in the form of a wind dragging the clouds along. BdKS attempted to develop a detailed model along these lines. Although they were able to obtain reasonable line profiles for certain sets of assumptions, the difficulties associated with confinement and survival of clouds dragged by a hot medium could not be satisfactorily addressed. This led them to suggest that confinement by magnetic fields instead of hot gas may be the only physically reasonable solution.

BAL models involving acceleration by UV resonance line radiation pressure were in fact among the first to be developed,

[1] Also at Department of Astrophysical, Planetary, and Atmospheric Sciences, University of Colorado, Boulder.

on the basis of the analogy between BAL profiles and P Cygni profiles that are observed from the winds of early-type stars (Drew & Boksenberg 1984). However, these models ran into problems, since they assumed that both the global covering factor and the filling factor of the absorbing material are 1 and that the gas provides its own confinement. In this case, unphysically large mass-loss rates are required, and many features of the observed line profiles cannot be reproduced. Consequently, this model was not generally accepted.

The case for acceleration by UV line radiation pressure was revived recently (Arav & Li 1994; Arav, Li, & Begelman 1994) by considering outflows with a very low filling factor of cool gas and a massless confining medium. Once these assumptions are made, this model is very successful in explaining observed BAL properties.

1. The momentum flux in the BAL clouds is very similar to the momentum absorbed from the radiation field in the BALs (see also Korista et al. 1992), as expected for winds that are not too optically thick.

2. Modeling the dynamics of such flows with techniques similar to those used for O-star winds shows (Arav & Li 1994; Arav et al. 1994) that a wind with the observed column densities reaches terminal velocities in the observed range if the flow starts at or just outside the BELR ($\sim 10^{18}$ cm).

3. Some objects show clear evidence of extra acceleration at velocities where the N v $\lambda 1240$ doublet starts to scatter Lyα emission-line photons, so that the emission line can contribute to the acceleration (Arav & Begelman 1994). Possible evidence for line-locking effects was also discussed by Weymann et al. (1991) and Korista et al. (1993).

The most outstanding observable difference between BAL QSOs and non-BAL QSOs that is not directly related to the lines themselves is the absence of radio-loud BAL QSOs (Stocke et al. 1992; Francis, Hooper, & Impey 1993). Some authors (Stocke et al. 1992) have argued that this must reflect an intrinsic difference between BAL and non-BAL QSOs, in which the same energy source that powers the jet in radio-loud objects gives rise to a fast wind in radio-quiet objects. This wind is then thought to be responsible for the BALs by stripping material from clouds. Some observational support for this picture is derived from the fact that BAL QSOs, although not radio-loud, still show radio emission that is consistent with what is expected from a wind. A competing hypothesis is that the absence of radio-loud BAL QSOs can be explained by selection effects resulting from beaming of the radio emission (de Kool 1993), under the assumption that the BALR is associated with the accretion disk and that BALs are only visible if our line of sight passes very close to the surface of the disk, i.e., perpendicular to a possible radio jet. This straightforwardly explains the absence of core-dominated radio-loud BAL QSOs. However, to explain the absence of extended, lobe-dominated radio-loud BAL QSOs, one has to make the additional assumption that the extended emission is also weakly beamed, and although this seems consistent with the observed distribution of the flux ratios between the lobes, this assumption is controversial. The beaming hypothesis avoids having to invoke ad hoc differences between BAL and non-BAL QSOs, which is attractive because, apart from the radio emission, there seems to be very little difference in QSO properties of BAL and non-BAL objects (e.g., Weymann et al. 1991). The accretion disk also seems a natural choice for the source of BAL material. Additional evidence that the BALR is only visible in QSOs where the line of sight is close to the accretion

disk comes from the polarization measurements of Glenn, Schmidt, & Foltz (1994).

Combining all the above considerations, a model for the BALR that ties it to the accretion disk and relies on magnetic confinement and acceleration by line radiation pressure seems attractive. In this paper we will explore such a model of a line radiation pressure–driven wind from a magnetized accretion disk. Note that this model has some similarities to the BELR model of Emmering, Blandford, & Shlosman (1992), which explains the BELs as resulting from a *hydromagnetically* driven disk wind. However, we shall show that the dynamical role of the magnetic field in our model is significantly different.

In § 2 of this paper we will give a general description of the model and make some order-of-magnitude estimates to show that the model is feasible. In § 3 we will present self-similar solutions of the simplified problem of optically thin winds and use these to illustrate the properties of such flows. Finally, in § 4 we will discuss our results.

2. DESCRIPTION OF THE MODEL

In Figure 1 we show a schematic representation of our BAL QSO model. At radii where the BAL outflow must originate (comparable to the radius of the BELR or beyond), the accretion disk is vertically self-gravitating and consequently must consist of a collection of relatively cool, mostly molecular clumps (e.g., Schlosman & Begelman 1989). Arguing along similar lines to Emmering et al. (1992), we assume that these clouds are threaded by a magnetic field, not unlike clouds in the interstellar medium in the disk of our Galaxy. Due to encounters or magnetic buoyancy, some clouds may acquire a small velocity perpendicular to the disk plane and become exposed to the UV radiation from the central source. As they emerge from the disk, they are immediately heated to a "warm" thermal equilibrium state, with temperatures $\sim 10^4$ K.

As shown below, we expect the magnetic field above the disk to be ordered, with mainly poloidal field lines. The heated cloud will be prevented from expanding sideways by the magnetic field and will expand mainly in the radial direction, forming a thin filament. In order to keep the cloud material confined, we have to assume that it is not completely optically thin in the radial direction so that the acceleration by radiation pressure can act as an effective gravity, compressing the cloud in the radial direction. In fact, the observed thickness of clouds in the radial direction ($\sim 10^{11}$ cm; see above) is a strong indication that the acceleration is ultimately responsible for the confinement: estimating the acceleration as $g_{\rm eff} \sim v^2/R$ with v and R the typical velocity and size of the BALR, it is easily shown that 10^{11} cm corresponds to about one scale height in a gas with the temperature of the BAL clouds ($\sim 3 \times 10^4$ K). Thus, we emphasize here that the small thickness of the BAL clouds is the natural size for clouds with a temperature of a few times 10^4 K being accelerated to velocities of $0.1c$ over a length scale of 10^{18} cm. This argument applies not only to radiative acceleration of optically thick clouds, but also to any mechanism that accelerates the clouds by a surface force, e.g., as in the model in which the clouds are dragged by a hot wind.

We will now estimate the relative magnitudes of the three main forces acting on a cloud: gravity, radiation pressure, and magnetic forces. The radiation force exerted on a gram of optically thin gas can be expressed as

$$F_{\rm rad} = F_{\rm grav}\left(\frac{L}{L_{\rm Edd}}\right)\left(\frac{\bar{\kappa}}{\kappa_{\rm T}}\right), \tag{2.1}$$
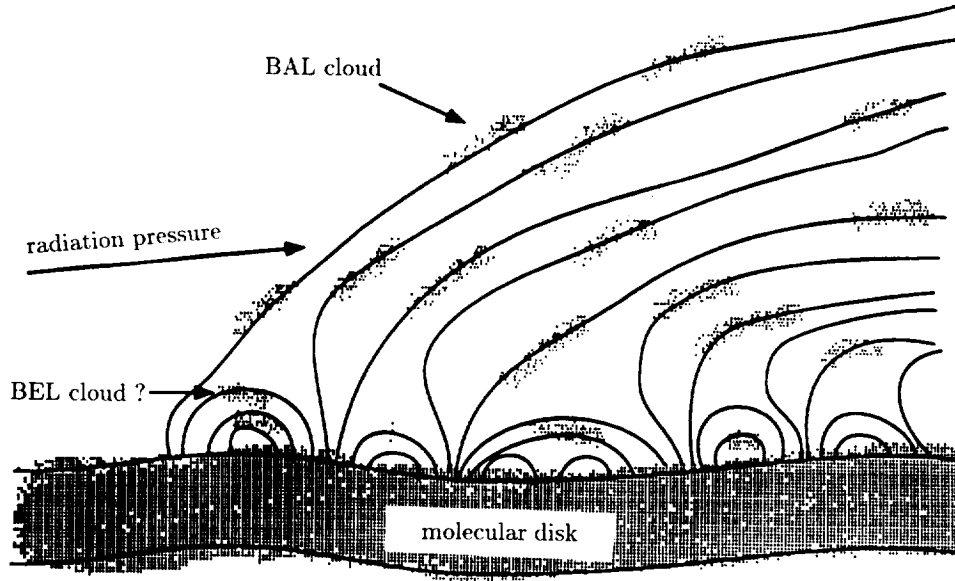
FIG. 1.—This figure illustrates the basic idea behind our model. Cool clouds that are threaded by magnetic field rise from the clumpy, self-gravitating accretion disk at a distance of $\sim 10^{18}$ cm^{-2} from the central black hole (e.g., as a result of gravitational scattering of clouds or from the Parker instability). As they are exposed to the continuum source, they are heated to a warm phase ($T \sim 10^4$ K) and rapidly accelerated outward by UV-line radiation pressure. The magnetic field carried by the flow is compressed against the disk up to the point where it becomes dynamically important, and the magnetic pressure gradient perpendicular to the disk forces the flow to spread to some opening angle $\phi_{\rm BAL}$. This occurs when the magnetic pressure is some significant fraction of the radiation pressure, so that the field is automatically strong enough to confine the BAL clouds at the required gas pressure.

where L is the QSO luminosity, $L_{\rm Edd}$ is the Eddington luminosity, κ_T is the Thomson opacity, and $\bar{\kappa}$ is the mean line opacity (averaged over the UV continuum). Because the opacity in UV resonance lines is so large relative to the Thomson opacity ($\bar{\kappa}/\kappa_T$ can be as large as 10^3 or 10^4; see, e.g., Arav & Li 1994; Arav et al. 1994), it is easy to show that the radiation force is much larger than gravity, provided that the luminosity of the QSO is $> 10^{-3}$ times the Eddington luminosity and that the cloud is not extremely optically thick ($N_H \sim 10^{20}$ cm^{-2}). Thus, all clouds with a column density below this limit will be accelerated outward, dragging the magnetic field along. Since the radiation force is much larger than gravity, the clouds will very quickly reach speeds far in excess of the local escape speed and the local Keplerian speed in the disk. This implies that the outflow will be almost purely poloidal and that the winding up of field lines with the development of a strong azimuthal field, which typifies hydromagnetically driven winds that are not subject to a strong radiation force (e.g., Blandford & Payne 1982; Emmering et al. 1992), will not occur.

Although the magnetic field lines will be combed out radially by the effect of radiation pressure, magnetic pressure forces will prevent the flow from being squashed flat against the disk. The

balance between magnetic and radiation forces will determine the thickness of the flow, yielding a flow geometry like that illustrated schematically in Figure 2. The magnetic force per unit mass, acting on the flow, is given by $F_{\rm mag} \sim \rho^{-1} P_{\rm mag}/d$, where d is the length scale over which the magnetic field changes (see Fig. 2) and $P_{\rm mag}$ is the magnetic pressure. We estimate the mean flow density by $\rho \sim \mu_H N_H/R$, where N_H is the hydrogen column density of the BALR. The corresponding force resulting from radiation pressure can be written in the form $F_{\rm rad} \sim \bar{\kappa} P_{\rm rad} = 400(\bar{\kappa}/10^3\kappa_T)P_{\rm rad}$, where $P_{\rm rad}$ is the radiation pressure. By demanding that in the equilibrium solution the magnetic and radiative forces must be comparable, we arrive at the estimate

$$\left(\frac{F_{\rm mag}}{F_{\rm rad}}\right) \sim \left(\frac{P_{\rm mag}}{P_{\rm rad}}\right)\left(\frac{R}{d}\right)N_{21}^{-1}\left(\frac{\bar{\kappa}}{10^3\kappa_T}\right)^{-1} \sim 1 , \qquad (2.2)$$

where N_{21} is the column density of the BALR normalized to 10^{21} cm^{-2}.

If we assume, in addition, that the magnetic field is responsible for the confinement of the BAL clouds, we must have $P_{\rm mag} \sim P_{\rm gas} \equiv \Xi^{-1} P_{\rm rad}$, where Ξ is the ionization parameter in a slightly different definition than that used for U above.
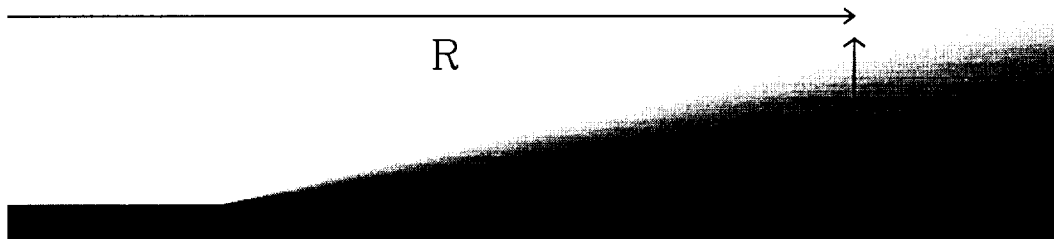

FIG. 2.—The geometry of the estimate leading to eq. (2.3)

The two are related by an expression of the form $\Xi = f(T)U$. Since we know P_{rad} from the QSO luminosity and Ξ from the ionization equilibrium ($\Xi_{\mathrm{BAL}} \sim 10$, e.g., Krolik, McKee, & Tarter 1981), we can estimate the magnetic pressure. Substituting $P_{\mathrm{mag}}/P_{\mathrm{rad}} \sim 0.1$ into equation (2.2) and solving for d/R, we obtain

$$\frac{d}{R} \sim 0.1 N_{21}^{-1}\left(\frac{\bar{\kappa}}{10^3 \kappa_{\mathrm{T}}}\right)^{-1} . \tag{2.3}$$

Thus, we can expect that clouds emerging from the disk are accelerated almost radially outward, compressing the magnetic field lines on which the clouds are moving up to a point where magnetic forces become comparable to the radiation force. Equation (2.3) indicates that for column densities in the range inferred from observations this will occur when the flow is compressed to a thickness $d \sim 0.01$–$0.3R$. Equation (2.3) is probably an underestimate, since we did not take account of the fact that the magnetic forces only need to balance the component of the radiation force perpendicular to the field lines. To give a more accurate estimate requires knowledge of the detailed shape of the field lines. In § 3, we shall derive the field line shape and flow opening angle from a rigorous analysis of a self-similar model.

Clearly, there are many uncertainties associated with this model that prevent us from constructing detailed models. Apart from the difficulties associated with two-dimensional line radiation transport, there are at present no reliable theoretical estimates available for the distribution of magnetic fields and mass loss over the surface of the accretion disk, the main quantities that will determine the structure of the flow. Because of this, we will only consider a very restricted class of models here, the self-similar ones (see Blandford & Payne 1982). The solutions we obtain in this case can be used to illustrate the properties of the kind of magnetic disk winds we are considering here.

3. SELF-SIMILAR SOLUTIONS FOR OPTICALLY THIN WINDS

3.1. The Basic Equations

We will consider azimuthally symmetric outflows in spherical geometry, where the toroidal components of the magnetic field and velocity are zero. In this way we neglect all effects of rotation of the underlying accretion disk, which is a good approximation since we have shown that the radial velocity of the wind will be much higher than the Keplerian speed. The equations of motion (in spherical polar coordinates) we want to solve are

$$\rho\left(v_r \frac{\partial v_r}{\partial r} + \frac{v_\theta}{r}\frac{\partial v_r}{\partial \theta} - \frac{v_\theta^2}{r}\right) = \rho a_{\mathrm{rad}}$$
$$+ \frac{1}{4\pi}\left(\frac{B_\theta}{r}\frac{\partial B_r}{\partial \theta} - \frac{B_\theta^2}{r} - B_\theta \frac{\partial B_\theta}{\partial r}\right), \tag{3.1a}$$

$$\rho\left(v_r \frac{\partial v_\theta}{\partial r} + \frac{v_\theta}{r}\frac{\partial v_\theta}{\partial \theta} + \frac{v_\theta v_r}{r}\right) = \frac{1}{4\pi}\left(-\frac{B_r}{r}\frac{\partial B_r}{\partial \theta} + \frac{B_\theta B_r}{r} + B_r \frac{\partial B_\theta}{\partial r}\right). \tag{3.1b}$$

To obtain self-similar solutions, we require that all quantities X can be written in the form

$$X = X_0 r^{-\alpha} \xi(\theta) ,$$

with X_0 a constant. For our optically thin wind approx-

imation, we take $a_{\mathrm{rad}} = a_0 r^{-2}$. Since the magnetic field is poloidal and divergence free, we can derive it from a potential, Ψ:

$$B_r = \frac{\sqrt{4\pi}}{r^2 \sin\theta}\frac{\partial \Psi}{\partial \theta} , \tag{3.2a}$$

$$B_\theta = \frac{-\sqrt{4\pi}}{r \sin\theta}\frac{\partial \Psi}{\partial r} . \tag{3.2b}$$

If we define $\Psi \equiv \Psi_0 r^{-\alpha} f(\theta)$, then

$$(B_r, B_\theta) = \frac{\Psi_0 \sqrt{4\pi}}{r^2 \sin\theta} r^{-\alpha}(f', \alpha f) , \tag{3.3}$$

where a prime denotes differentiation with respect to θ. If we define $\Psi(0, \pi/2) = 0$, then $\Psi(R, \pi/2)$ is proportional to the total magnetic flux through the surface of the disk for radii smaller than R, and we see that α has to be negative. From the condition that all terms in equation (3.1a) scale with the same power of r, we obtain that $v \propto r^{-1/2}$ and $\rho \propto r^{-(3+2\alpha)}$. Mass conservation states that ρv is divergence free and can also be derived from a potential, χ:

$$(\rho v)_r = \frac{\sqrt{4\pi}}{r^2 \sin\theta}\frac{\partial \chi}{\partial \theta} , \tag{3.4a}$$

$$(\rho v)_\theta = \frac{-\sqrt{4\pi}}{r \sin\theta}\frac{\partial \chi}{\partial r} , \tag{3.4b}$$

where $\chi(R, \pi/2)$ is proportional to the integrated mass flux from the surface of the disk for $r < R$. Since flux-freezing implies that the velocity is always parallel to the magnetic field, lines of constant χ must coincide with lines of constant Ψ, implying

$$\chi = \chi(\Psi) \equiv b\Psi^\beta . \tag{3.5}$$

Substituting the scalings of v and ρ obtained above into equation (3.4a) and using equation (3.5), we find that self-similar solutions exist only if $\beta = 2 + (3/2\alpha)$. Thus, for a prescribed distribution of magnetic flux over the surface of the disk, self-similar solutions exist only for one distribution of mass flux from the disk.

In addition to $f(\theta)$, there is one more free angular function which needs to be calculated, which we define in terms of the density. Let

$$\rho \equiv r^{-(3+2\alpha)}\frac{f^{\beta-1}(\theta)}{g(\theta)\sin\theta} . \tag{3.6}$$

This strange-looking definition will lead to more compact equations. Substituting this into equations (3.4a)–(3.4b), we obtain

$$(v_r, v_\theta) = \Psi_0^\beta br^{-1/2}\beta g(f', \alpha f) . \tag{3.7}$$

An energy equation can be constructed by multiplying equation (3.1a) by $1/\rho$ and equation (3.1b) by $B_\theta/(\rho B_r)$ and adding the two, leading to

$$a_{\mathrm{rad}} = \frac{1}{2}\frac{\partial}{\partial r}(v_r^2 + v_\theta^2) + \frac{v_\theta}{2rv_r}\frac{\partial}{\partial \theta}(v_r^2 + v_\theta^2) . \tag{3.8}$$

The magnetic terms cancel because they do no work on the flow. Canceling factors of r^{-2} and rearranging terms after substituting equation (3.7) into equation (3.8), we can write

equation (3.8) in the form

$$\frac{2a_0}{\Psi_0^{2\beta}b^2\beta^2} + g^2[(f')^2 + \alpha^2 f^2] = \alpha \frac{f}{f'} \frac{\partial}{\partial\theta}$$

$$\times \left\{ \frac{2a_0}{\Psi_0^{2\beta}b^2\beta^2} + g^2[(f')^2 + \alpha^2 f^2] \right\} , \quad (3.9)$$

where we have used the fact that $2a_0/(\Psi_0^{2\beta}b^2\beta^2)$ is a constant. Equation (3.9) is easily integrated. To fix the constant of integration, let us consider flows that start from rest at the disk ($\theta = \pi/2$), with f and f' finite. Therefore, we have $g(\pi/2) = 0$, and we may arbitrarily take $f(\pi/2) = 1$. In this case, integrating equation (3.9) yields

$$1 + \frac{\Psi_0^{2\beta}b^2\beta^2}{2a_0} g^2[(f')^2 + \alpha^2 f^2] = f^{1/\alpha} . \quad (3.10)$$

Equation (3.10) is the self-similar form of the energy equation. Next, substituting equations (3.2a)–(3.2b), (3.4a)–(3.4b), and (3.6) into equation (3.1b), we obtain

$$\Psi_0^{2\beta-2}b^2\beta^2\alpha f^\beta \left[\frac{\partial}{\partial\theta} (\alpha g f) + \frac{g f'}{2} \right]$$

$$= -f' \left[\frac{(1+\alpha)\alpha f}{\sin\theta} + \frac{\partial}{\partial\theta} \left(\frac{f'}{\sin\theta} \right) \right] . \quad (3.11)$$

Defining the new variables

$$y \equiv f^{-(1/\alpha)} , \quad w \equiv \frac{\Psi_0 \beta b \alpha\beta}{\sqrt{2a_0}} g f^{1+(1/2\alpha)} , \quad (3.12)$$

equation (3.10) becomes

$$(1 - y) - w^2(y^2 + y'^2) = 0 , \quad (3.13)$$

and equation (3.11 becomes)

$$\frac{\Psi_0^{\beta-2}b\beta\sqrt{2a_0}}{\alpha} \sin\theta \frac{w'}{y'}$$

$$= (\alpha + 1)\left[1 + \left(\frac{y'}{y}\right)^2 \right] + \frac{\cos\theta}{\sin\theta} \frac{y'}{y} - \frac{y''}{y} . \quad (3.14)$$

Using equation (3.13), we eliminate w from equation (3.14) (taking the negative root, since eq. [3.12] implies that w is negative) to obtain a second-order ordinary differential equation for y,

$$y'' \left[1 - \frac{2C_0 \sin\theta(1-y)^{1/2}y}{(y^2 + y'^2)^{3/2}} \right] = \frac{C_0 \sin\theta(1-y)^{1/2}}{(y^2 + y'^2)^{1/2}}$$

$$\times \left[\frac{2y^2}{(y^2 + y'^2)} + \frac{y}{1-y} \right] + \frac{\cos\theta}{\sin\theta} y' + (1+\alpha)y \left[1 + \left(\frac{y'}{y}\right)^2 \right] .$$

$$(3.15)$$

We see that the solution depends only on the constants α and C_0, the latter being given by

$$C_0 \equiv -\frac{\alpha + (3/4)}{\alpha^2} \Psi_0^{3/2\alpha}b\sqrt{2a_0} . \quad (3.16)$$

The equation requires two boundary conditions. The first one has already been used to derive equation (3.10): $f(\pi/2) = 1$, implying $y(\pi/2) = 1$. For the second condition, we have a choice. We can prescribe y' at the surface of the disk, which

turns the solution into an initial value problem. This is equivalent to prescribing the angle the field lines have with respect to the disk plane when they emerge from the disk. Alternatively, we can demand that the flow be confined to a region between the disk and a minimum angle θ_b, i.e., we demand $y(\theta_b) = 0$, in which case we have to solve a two-point boundary value problem. The solutions of equation (3.15) can contain critical points when the velocity component in the θ direction becomes equal to the Alfvén speed:

$$\frac{2C_0 \sin\theta(1-y)^{1/2}y}{(y^2 + y'^2)^{3/2}} = \frac{4\pi\rho v_\theta^2}{B_r^2 + B_\theta^2} \equiv M_\theta^2 = 1 . \quad (3.17)$$

The same type of critical point also occurs in the self-similar hydromagnetic wind models of Blandford & Payne (1982).

3.2. Solutions: General Constraints

We are interested in solutions of equation (3.15) in which the magnetically confined outflow takes place between the disk and a minimum angle θ_b. The range of parameters that will lead to physically acceptable solutions can be limited by considering the behavior at the boundary θ_b. In order to match to the vacuum, the magnetic pressure at the boundary must vanish, implying $f(\theta_b) = f'(\theta_b) = 0$. Moreover, the field must be parallel to the boundary, implying $f/f' \to 0$ as $\theta \to \theta_b$. In terms of the variable y, we have (for $\alpha < 0$)

$$y(\theta_b) = 0 , \quad \frac{y}{y'} \to 0 \quad \text{as} \quad \theta \to \theta_b . \quad (3.18)$$

Making these substitutions in equation (3.15) and retaining only the leading terms, we have

$$y'' \left(1 - \frac{2C_0 \sin\theta y}{y'^3} \right) = \frac{C_0 \sin\theta y}{y'} \left(\frac{2y}{y'^2} + 1 \right)$$

$$+ \frac{\cos\theta}{\sin\theta} y' + (1+\alpha) \frac{y'^2}{y} . \quad (3.19)$$

If y'' is finite at the boundary, we can make a Taylor expansion around the boundary to study the behavior of the solution there. However, when doing so it is easily seen that this approximate solution implies that $y'' \to \infty$ at the boundary, showing that the assumption of finite y'' is inconsistent. Thus, we expand the solution in $\Delta = \theta - \theta_b$ by assuming that

$$y'' \to A\Delta^{-\mu} \quad \text{as} \quad \theta \to \theta_b . \quad (3.20)$$

Since we want f and f' to go to zero at the boundary, the singularity in y'' must be integrable, leading to the constraint that $0 < \mu < 1$. Then, substituting into equation (3.19) that

$$y' \to \frac{A}{1-\mu} \Delta^{1-\mu} , \quad y \to \frac{A}{(1-\mu)(2-\mu)} \Delta^{2-\mu} , \quad (3.21)$$

we obtain

$$\left[1 - \frac{2C_0 \sin\theta_b}{A^2} \frac{(1-\mu)^2}{2-\mu} \Delta^{2\mu-1} \right]$$

$$= \frac{\cos\theta_b}{\sin\theta_b} \frac{\Delta}{1-\mu} + (1+\alpha) \frac{2-\mu}{1-\mu} . \quad (3.22)$$

It is impossible to satisfy the equation (3.22) when $\mu < \frac{1}{2}$. If $\mu > \frac{1}{2}$, we have $\Delta^{2\mu-1} \to 0$, implying

$$\mu = \frac{1 + 2\alpha}{\alpha} , \quad (3.23)$$

and $-1 < \alpha < -\frac{2}{3}$. If $\mu = \frac{1}{2}$ identically, equation (3.22) reduces to

$$\frac{C_0 \sin \theta_b}{3A^2} = -(2 + 3\alpha) , \qquad (3.24)$$

and because the left-hand side of equation (3.23) is positive, we must have $\alpha < -\frac{2}{3}$.

We constrain the solutions further by demanding that the density go to zero at the boundary, or $\rho(\theta_b) = 0$. We have

$$\rho \propto f^{\beta-1} g^{-1} \propto \Delta^{(1-\mu)-2(\alpha+1)(2-\mu)} . \qquad (3.25)$$

If equation (3.23) applies, we have $\rho \propto \Delta^{-(1-\mu)} \to \infty$, so we reject this solution, and the solution with $\mu = \frac{1}{2}$ is the only remaining one. For this solution, we find from equation (3.25) that the density at the boundary goes to zero as long as $\alpha < -\frac{5}{6}$.

3.3. Scaling of the Solutions for Highly Compressed Flows

Consider the basic equation (3.15). When the radiation pressure is very strong, or equivalently the constant C_0 is large, the flow will be confined to a narrow wedge over the suface of the disk. In this case, we can expect that $y' \gg y$. Using this approximation, changing the independent variable from θ to $x \equiv C_0^{1/3}[\pi/2 - \theta]$ and taking $\sin \theta \approx 1$ and $\cos \theta \approx x C_0^{1/3}$, equation (3.15) can be written as

$$\ddot{y}\left[1 - \frac{2y(1-y)^{1/2}}{\dot{y}^3}\right] = \frac{(1-y)^{1/2}}{\dot{y}}\left(C_0^{-2/3}\frac{2y^2}{\dot{y}^2} + \frac{y}{1-y}\right)$$
$$+ C_0^{-2/3}x\dot{y} + (1 + \alpha)\frac{\dot{y}^2}{y} , \qquad (3.26)$$

where an overdot represents differentiation with respect to x. Now suppose that x and all the dotted derivatives of y are of order 1, and that C_0 is large. Then the terms containing $C_0^{-2/3}$ can be neglected in equation (3.26), leading to

$$\ddot{y}\left[1 - \frac{2y(1-y)^{1/2}}{\dot{y}^3}\right] = \frac{y}{\dot{y}(1-y)^{1/2}} + (1 + \alpha)\frac{\dot{y}^2}{y} . \qquad (3.27)$$

Once this equation is solved, the solution for a given C_0 can be determined by scaling the solution with the transformation $\theta = (\pi/2) - C_0^{-1/3}x$. In this limit, the opening angle of the outflow $\phi_{BAL} \equiv (\pi/2) - \theta_b$ will scale with $C_0^{-1/3}$. The numerical solutions below show that this scaling is quite accurate for $C_0 > 1$.

3.4. A Numerical Solution

We will now present a numerical solution of equation (3.15) to show the character of the solutions. Consider the case $\alpha = -1$. This choice for α is inspired by the observation that the ionization parameter of BAL outflows does not vary strongly with outflow velocity, so that the magnetic pressure responsible for confinement should scale as r^{-2}, which in our model implies $\alpha = -1$.

To solve equation (3.15) (note that for $\alpha = -1$ the last term on the right-hand side vanishes) we need two boundary conditions. The first one is that $y = 0$ at the disk surface. For the second one we use the result of our discussion in § 3.2 that at the boundary θ_b, y behaves as in equation (3.21) with $\mu = \frac{1}{2}$ and A given by equation (3.24). The location of θ_b is not known a priori. For $\alpha = -1$ and $\mu = \frac{1}{2}$, the right-hand side of equation (3.22) vanishes for $\Delta \to 0$, so that the left-hand side must also vanish, implying that the boundary point θ_b is also a critical point.

The numerical solution for a given C_0 is determined by shooting from the two boundaries to an interior fitting point. Taking first guesses for y' at the disk surface and for the location of θ_b, we integrate equation (3.15) outward from the disk and inward from θ_b, in the latter case using the expansion in equation (3.21) for the first integration step because y'' diverges there. The correct solution is now found by iterating this procedure until the values of y' at the disk surface and θ_b are such that the two solutions match at an interior fitting point.

Figure 3 shows the shape of the field lines obtained for $C_0 = 1$. The straight line from the origin is the limiting angle θ_b, which for $C_0 = 1$ has the value 0.552. In Figure 4 we illustrate the runs of the Mach number M_θ defined in equation (3.17), the density, and the magnetic pressure with θ for a given radius. In Figure 5 the opening angle of the outflow ϕ_{BAL} is plotted as a function of C_0, clearly illustrating that the scaling law $\phi_{BAL} \propto C_0^{-1/3}$ is a very good approximation for $C_0 > 1$.

3.5. Physical Scales

In this section we will investigate whether the model described above can yield the observed quantitative properties of the BAL region. We want to express the constant C_0 in more easily interpretable physical quantities. For simplicity, we will again constrain ourselves to models with $\alpha = -1$. First we determine a physical value for the constant a_0 giving the strength of the radiation pressure

$$a_0 = GM_{BH}\left(\frac{\bar{\kappa}}{\kappa_T}\right)\left(\frac{L}{L_{Edd}}\right) \approx 10^{36}M_8 \mathcal{M}_3 \mathcal{L}_{-1} \text{ (cgs)} , \qquad (3.28)$$

where M_8 is the mass of the central black hole in units of 10^8 $M_\odot$, $\mathcal{M}_3$ is $\bar{\kappa}/\kappa_T$ in units of 10^3, and $\mathcal{L}_{-1}$ is the luminosity in units of $0.1L_{Edd}$. Using the fact that $4\pi^{3/2}\Psi(R)$ is the magnetic flux through the surface of the disk integrated from $r = 0$ to $r = R$, and that the largest contribution to this integral comes
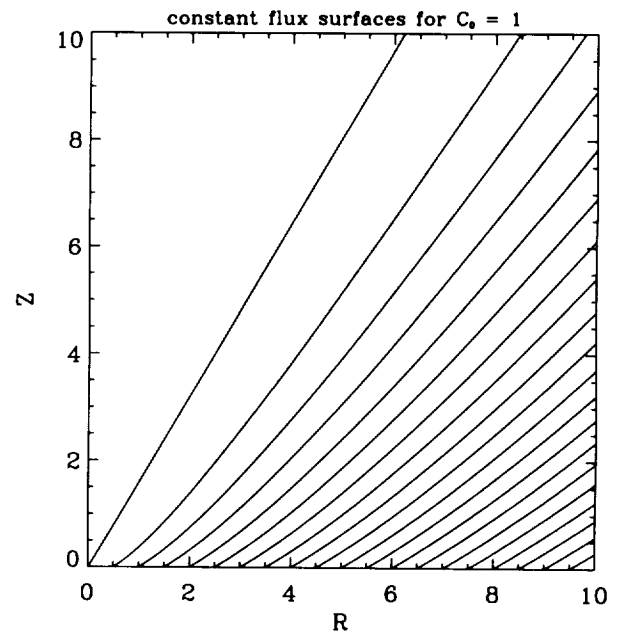

FIG. 3.—The shape of the compressed field lines for a model with $\alpha = -1$ and $C_0 = 1$. The straight line coming from the origin shows the boundary angle, which is $\theta_b = 0.552$ for these parameters.
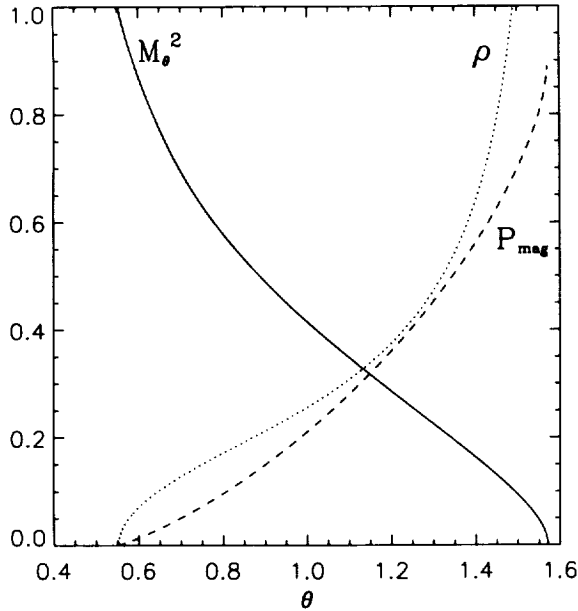
FIG. 4.—The run of density ρ, magnetic pressure P_{mag}, and Mach number M_θ as a function of θ. The density and magnetic pressure are arbitrarily normalized. The density goes to infinity in the disk plane, i.e., for $\theta = \pi/2$.

from $r \approx R$, we have $\Psi = [(4\pi)^{1/2}]^{-1}R^2 B_\theta$, and we can estimate

$$\Psi_0 \approx \frac{RB_\theta}{\sqrt{4\pi}} . \qquad (3.29)$$

Similarly, $4\pi^{3/2}\chi$ is the integrated mass loss from the disk for $r < R$, so that from equation (3.5) we have

$$b = \frac{\chi}{\Psi^{1/2}} \approx 0.1 \frac{\dot{M}}{RB_\theta^{1/2}} . \qquad (3.30)$$

Substituting these expressions for a_0, Ψ_0, and b into the definition of C_0, we obtain

$$C_0 \approx 100\dot{M}_{26} R_{18}^{-5/2}B_{\theta,-2}^{-2}M_8^{1/2} \mathcal{M}_3^{1/2} \mathscr{L}_{-1}^{1/2} , \qquad (3.31)$$

with $\dot{M}_{26}$ the mass-loss rate in units of 10^{26} g s^{-1}, R_{18} the radius of the BALR normalized to 10^{18} cm, and $B_{\theta,-2}$ the vertical component of the magnetic field at the disk surface in units of 10^{-2} G. Estimating $(f'/f) \approx \phi_{\rm BAL}^{-1} \approx C_0^{1/3}$ at the disk surface, the total magnetic pressure becomes

$$P_{mag} \equiv \frac{B_\theta^2 + B_r^2}{8\pi} = \frac{B_\theta^2}{8\pi}\left[1 + \left(\frac{f'}{f}\right)^2\right] \approx \frac{B_\theta^2}{8\pi}(1 + C_0^{2/3}) . \qquad (3.32)$$

If we require the magnetic pressure to be of the order of the gas pressure in BAL clouds, $P_{mag} \sim P_{\rm BAL} \sim 10^{-4}M_8\mathscr{L}_{-1}R_{18}^{-2}$ dyn cm^{-2}, and take $C_0 > 1$, we obtain

$$\phi_{\rm BAL} \approx 0.1\dot{M}_{26}^{-1} R_{18}^{1/2} M_8^{1/2} \mathcal{M}_3^{-1/2} \mathscr{L}_{-1}^{1/2} . \qquad (3.33)$$

From equation (3.33), we see that these simple assumptions lead to the conclusion that a rather high mass-loss rate of the order of 1 $M_\odot$ yr^{-1} is needed to explain the observed covering factor of the BALR. Although a mass-loss rate of this order is not unreasonable in comparison with the accretion rate inferred for the central black hole, it is at the upper end of what the UV line profiles indicate. It could also lead to more optically thick winds, in which the effective opacity would be
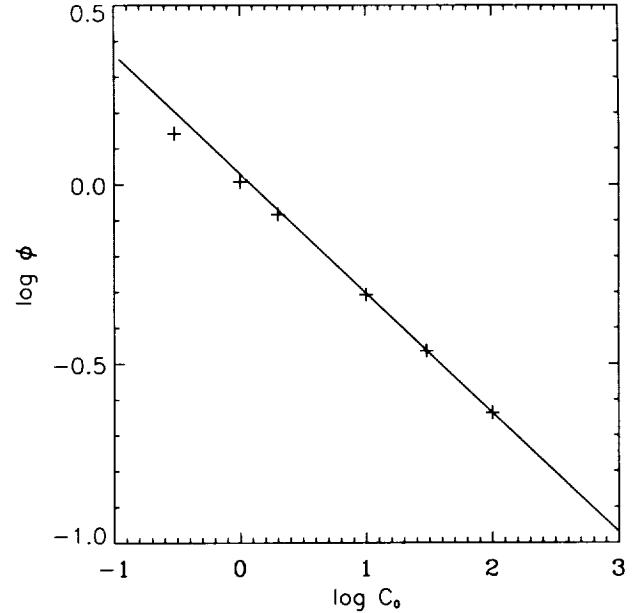

FIG. 5.—The scaling of the opening angle of the outflow $\phi_{\rm BAL} \equiv (\pi/2) - \theta_b$ with the parameter C_0. The straight line is a line with slope $-\frac{1}{3}$; the crosses are calculated by solving the full eq. (3.15) for different values of C_0. It is seen that the scaling derived for $C_0 \gg 1$ is quite good even outside its formal range of validity.

reduced below the value used in equation (3.33), thus increasing $\phi_{\rm BAL}$ again.

A straightforward way out of this problem is to assume that the ionizing flux that determines the pressure in the BALR is smaller than would be expected from a simple extrapolation of the UV flux that does the line driving. It is easy to show that a reduction of the number of ionizing photons enters linearly into the expression $\phi_{\rm BAL}$, so that a reduction of this flux by a factor of 10 caused by some highly ionized absorber would suffice to obtain the correct opening angle for a mass-loss rate of 0.1 $M_\odot$ yr^{-1}, in much better agreement with observed BAL profiles. Evidence for the existence of such highly ionized absorbers with the necessary column density ($N_H \sim 10^{20}$–10^{22} cm^{-2}) is seen in the X-ray spectra of several Seyfert galaxies (Netzer 1993; Netzer, Turner, & George 1995).

4. DISCUSSION

In this paper we have studied a very simple model of a radiatively driven magnetic disk wind that could be a general feature of all high-luminosity QSOs. Clearly the simplifications are so severe that we cannot make detailed predictions about line profiles, ionization states, etc. However, some general properties of our models, such as the fact that the observed opening angle of the BAL outflow can be reproduced for a reasonable set of physical parameters, can be expected to apply in more detailed models as well.

Several other observed features of BAL QSOs seem to fit naturally into our model. The model predicts that as the line of sight to the continuum source makes a smaller angle with respect to the disk surface, it passes through regions with a smaller ratio of radiation pressure to magnetic (i.e., confining) pressure, implying a lower ionization parameter. This suggests that the appearance of a QSO may change from a high-ionization BAL QSO to a low-ionization BAL QSO as the angle between the line of sight to the center and the disk gets

smaller. Some observational characteristics of low-ionization BAL QSOs, such as their large infrared-to-optical flux ratios (Low et al. 1989) and the evidence for dust absorption in their spectra (Sprayberry & Foltz 1992), lend support to this picture.

The model also provides an explanation for the finding of Voit, Weymann, & Korista (1993) that, based on ionization equilibrium calculations, the high-velocity material is shielding the lower velocity, lower ionization gas in the line of sight to the central continuum source. Such a situation, with the high-velocity gas being closer to the center than the low-velocity gas, is exactly what is predicted by the radiatively accelerated disk wind model.

Recently a new model for BAL QSOs was proposed by Murray et al. (1995), which attempts to explain the BALs using a radiatively driven disk wind with a filling factor of one, i.e., without any clouds. The great advantage of such a model is that one does not have to deal with the problems associated with the confinement and survival of the very small BAL clouds, and it would obviate the need for any magnetic fields in the outflow. However, to construct a model with a continuous wind it was necessary to make two assumptions that deviate strongly from the "standard" model. The first is that the size of the BALR is about a factor of 100 smaller than the scales considered here, and the second is that the ionization parameter in the BALR is about 100 times larger. To reconcile the latter with the observed ionization state of the BALR, a very highly ionized and high column density ($N_H \sim 10^{24}$ cm^{-2}) absorbing screen is assumed to exist between the central continuum source and the BALR.

In our opinion, this has at least two consequences that are very difficult to reconcile with observations. First, the small scale of the BALR required by Murray et al. ($\sim 10^{16}$ cm) makes it very hard to explain the observed lack of variability in the BAL profiles on a timescale of several years (Barlow, Junkkarinen, & Burbidge 1989; Barlow et al. 1992), since the crossing time of the BALR would be of the order of months. Since most observed BAL profiles are highly structured, such changes on the flow timescale should be easily observable. Even if the structure we see is caused by some structure in the disk influencing the mass loss, so that the flow crossing timescale is not relevant, the rotation period of the structures on the disk would still be shorter than the timescales over which no variability is observed. Second, although the class of BAL QSOs as a whole may be underluminous in X-rays (Green et al. 1995), the strong X-ray shielding of the BAL outflow required in this case to avoid overionizing the wind does not

seem consistent with the fact that several BAL QSO have been observed with normal optical-to-X-ray flux ratios (Bregman 1984; Gioia et al. 1986; Singh, Westergaard, & Schnopper 1987; de Kool & Meurs 1994; Green et al. 1995).

From the theoretical side, some aspects of the model also need closer study. It is not clear that the hard ionizing flux can be suppressed as strongly as needed in the model, since a large fraction of the absorbed energy will be reemitted in the soft X-ray band (Netzer 1993). Since the evidence that the BALR coincides with or lies outside the BELR is incontrovertible, the model also implies that the BELR lies at much smaller radii than previously thought and will have to be ionized by a heavily absorbed spectrum. Attempts at modeling the observed ionization state of the BELR with such ionizing spectra have not been very successful so far (H. Netzer, private communication).

While a model invoking clouds is necessarily more complicated, we are unconvinced that it is inherently less plausible than a continuous wind model, especially in light of the difficulties mentioned above. In arguing the disadvantages of the cloud model, Murray et al. claim that there are no physical effects which would set a size scale for clouds. However, we have shown (§ 2) that the inferred sizes of BAL clouds coincide with the pressure scale height of the absorbing gas in the accelerating reference frame of the wind. Thus, very small cloud sizes may be a generic feature of any BAL wind model in which the accelerating force is mainly applied at the surface of the absorbing material. This would include radiative acceleration of clouds with moderate to high optical depths, as well as dragging of clouds by magnetic stresses or a hot intercloud medium.

The magnetized wind model proposed by us may be difficult to extend to the point at which a detailed comparison with observations is possible, but it does not lead to clear contradiction with observation, and it does not require us to revise the currently accepted picture of QSO structure. Further theoretical investigations are clearly necessary, especially regarding the details of the magnetic confinement mechanism, and we are currently investigating this issue.

REFERENCES

Arav, N., & Begelman, M. C. 1994, ApJ, 434, 479
Arav, N., & Li, Z. 1994, ApJ, 427, 700
Arav, N., Li, Z., & Begelman, M. C. 1994, ApJ, 432, 62
Barlow, T. A., Junkkarinen, V. T., & Burbidge, E. M. 1989, ApJ, 347, 674
Barlow, T. A., Junkkarinen, V. T., Burbidge, E. M., Weymann, R. J., Morris, S. L., & Korista, K. T. 1992, ApJ, 397, 81
Begelman, M. C., de Kool, M., & Sikora, M. 1991, ApJ, 382, 416 (BdKS)
Blandford, R. D., & Payne, D. G. 1982, MNRAS, 199, 883
Bregman, J. N. 1984, ApJ, 276, 423
de Kool, M. 1993, MNRAS, 265, L17
de Kool, M., & Meurs, E. J. A. 1994, A&A, 281, L65
Drew, J. E., & Boksenberg, A. 1984, MNRAS, 211, 813
Emmering, R. T., Blandford, R. D., & Shlosman, I. 1992, ApJ, 385, 460
Francis, P. J., Hooper, E. J., & Impey, C. D. 1993, AJ, 106, 417
Gioia, I. M., Maccacaro, T., Schild, R. E., Giommi, P., & Stocke, J. T. 1986, ApJ, 307, 497
Glenn, J., Schmidt, G. D., & Foltz, C. B. 1994, ApJ, 434, L47
Green, R., et al. 1995, ApJ, in press
Hamann, F., Korista, K. T., & Morris, S. L. 1993, ApJ, 415, 541
Korista, K. T., et al. 1992, ApJ, 401, 529

Korista, K. T., Voit, G. M., Morris, S. L., & Weymann, R. J. 1993, ApJS, 88, 357
Krolik, J. H., McKee, C. F., & Tarter, C. B. 1981, ApJ, 249, 422
Low, F. J., Cutri, R. M., Kleinmann, S. G., & Huchra, J. P. 1989, ApJ, 340, L1
Murray, N., Chiang, J., Grossman, S. A., & Voit, G. M. 1995, ApJ, 451, 498
Netzer, H. 1993, ApJ, 411, 594
Netzer, H., Turner, T. J., & George, I. M. 1995, ApJ, 435, 106
Shlosman, I., & Begelman, M. C. 1989, ApJ, 341, 685
Singh, K. P., Westergaard, N. J., & Schnopper, H. W. 1987, A&A, 172, L1
Sprayberry, D., & Foltz, C. B. 1992, ApJ, 390, 39
Stocke, J. T., Morris, S. L. Weymann, R. J., & Foltz, C. B. 1992, ApJ, 396, 487
Turnshek, D. A. 1988, in QSO Absorption Lines: Probing the Universe, ed. S. C. Blades, D. A. Turnshek, & C. A. Norman (Cambridge: Cambridge Univ. Press), 17
Voit, G. M., Weymann, R. J., & Korista, K. T. 1993, ApJ, 413, 95
Weymann, R. J., Morris, S. L., Foltz, C. B., & Hewett, P. C. 1991, ApJ, 373, 23
Weymann, R. J., Turnshek, D. A., & Christiansen, W. A. 1985, in Astrophysics of Active Galaxies and Quasi-stellar Objects, ed. J. Miller (Oxford: Oxford Univ. Press), 333 (WTC)